ResearchGate

See discussions, stats, and author profiles for this publication at: https://www.researchgate.net/publication/307594745

High-Performance Field-Effect Transistors Fabricated with Donor– Acceptor Copolymers Containing S···O...

Article *in* Macromolecules · September 2016

DOI: 10.1021/acs.macromol.6b01510

CITATIONS
7

READS
38

5 authors, including:

Weifeng Zhang
Chinese Academy of Sciences
53 PUBLICATIONS **401** CITATIONS
SEE PROFILE

Jianyao Huang
Chinese Academy of Sciences
36 PUBLICATIONS **253** CITATIONS
SEE PROFILE

Dong Gao
Chinese Academy of Sciences
24 PUBLICATIONS **514** CITATIONS
SEE PROFILE

Weiping Wu
University of Cambridge
184 PUBLICATIONS **5,155** CITATIONS
SEE PROFILE

Some of the authors of this publication are also working on these related projects:

organic optoelectronic materials and devices View project

conjugated materials and magnetic properties View project

All content following this page was uploaded by Weifeng Zhang on 04 September 2016.

The user has requested enhancement of the downloaded file.

Macromolecules

Article

pubs.acs.org/Macromolecules

High-Performance Field-Effect Transistors Fabricated with Donor−Acceptor Copolymers Containing S···O Conformational Locks Supplied by Diethoxydithiophenethenes

Weifeng Zhang,[†] Zupan Mao,[†] Jianyao Huang, Dong Gao, and Gui Yu*

Institute of Chemistry, Beijing National Laboratory for Molecular Sciences, Chinese Academy of Sciences, Beijing 100190, P. R. China

Supporting Information

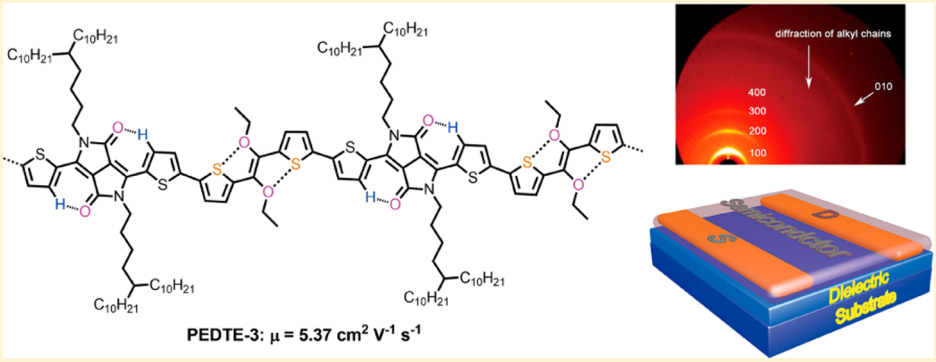

ABSTRACT: Constructing planar π-conjugated backbone is of critical importance for polymeric semiconductors to obtain high charge carrier mobility. In this regard, suitable introduction of noncovalent interactions is one of useful approaches. Herein, we report a series of donor−acceptor copolymers based on diethoxydithiophenethene (EDTE), namely PEDTE*n* (*n* = 1, 2, and 3), containing multiple O···H−C and S···O conformational locks, where the latter ones are supplied by the EDTE units. PEDTE*n* owns planar conjugated backbones with suitable HOMO energy levels (ca. − 5.20 eV) and strong absorption behaviors along with enhanced solution processability. High-performance field-effect transistors based on the copolymers exhibited a high hole mobility of up to 5.37 $cm^2\ V^{-1}\ s^{-1}$, which is among the highest values of semiconducting polymers based on the concept of conformational locks. AFM and GIXRD experiments reveal that PEDTE*n* could form crystalline and close packing thin films with a π−π stacking distance of down to 3.78 Å.

INTRODUCTION

Semiconducting polymers have received extensive attention because of their adjustable optoelectronic properties, good compatibility with flexible substrates, and excellent solution processability.[1−3] These inherent advantages endow the kind of organic semiconductors with great potentials to realize various flexible electronic devices, such as organic photovoltaics[4−9] and organic field-effect transistors (OFETs) via cost-effective graphic art printing processes.[10−14] OFETs are the essential components for the next generation of organic circuits that can be used as radio frequency identification cards, memories, sensors, and drivers for flexible displays.[15−18] In recent years, the research of polymer field-effect transistors (PFETs), in which semiconducting polymers are used as *p*- and/or *n*-type charge carrier transport materials, has made great progress. Some polymers even exhibited high mobilities of close to or exceeding 10 $cm^2\ V^{-1}\ s^{-1}$.[19−23] However, the device performances including current-carrying capacity, thermal stability, and device stability etc., even mobility are still far behind the actual requirement for realizing practical application of PFETs. Therefore, further discovering new high-performance polymeric semiconductors and understanding of the structure−property relationship are still highly necessary.

It is well-recognized that highly planar π-conjugated backbone is beneficial to obtain close π−π stacking, high frontier orbital overlap integrals, and thus afford high charge carrier mobility.[24−28] Hence, the strategy of designing planar building blocks acting as donor (D) or acceptor (A) units to develop D−A copolymers has been adopted, where close π−π stacking is always afforded resulting from the push−pull effect between donor and acceptor units.[29−40] Among numerous building blocks, diketopyrrolopyrrole (DPP) is the most famous one because most of the record high mobilities have been obtained by D−A copolymers containing DPP units during recent years.[21−23] Nielsen et al. theoretically predicted the conformation of dithienyl-DPP by Gaussian B3LYP/6-31G* level, suggesting that the small dihedral angles (12°) between DPP and thiophene units may be originated from the

Received: July 13, 2016
Revised: August 23, 2016

ACS Publications © XXXX American Chemical Society

DOI: 10.1021/acs.macromol.6b01510
Macromolecules XXXX, XXX, XXX−XXX

Scheme 1. (a) Chemical Structures and Synthetic Routes of PEDTE*n* (*n* = 1, 2, and 3) and (b) Schematic Noncovalent O···H−C and S···O Conformational Locks in Conjugated Backbones of EDTE-Based Polymers

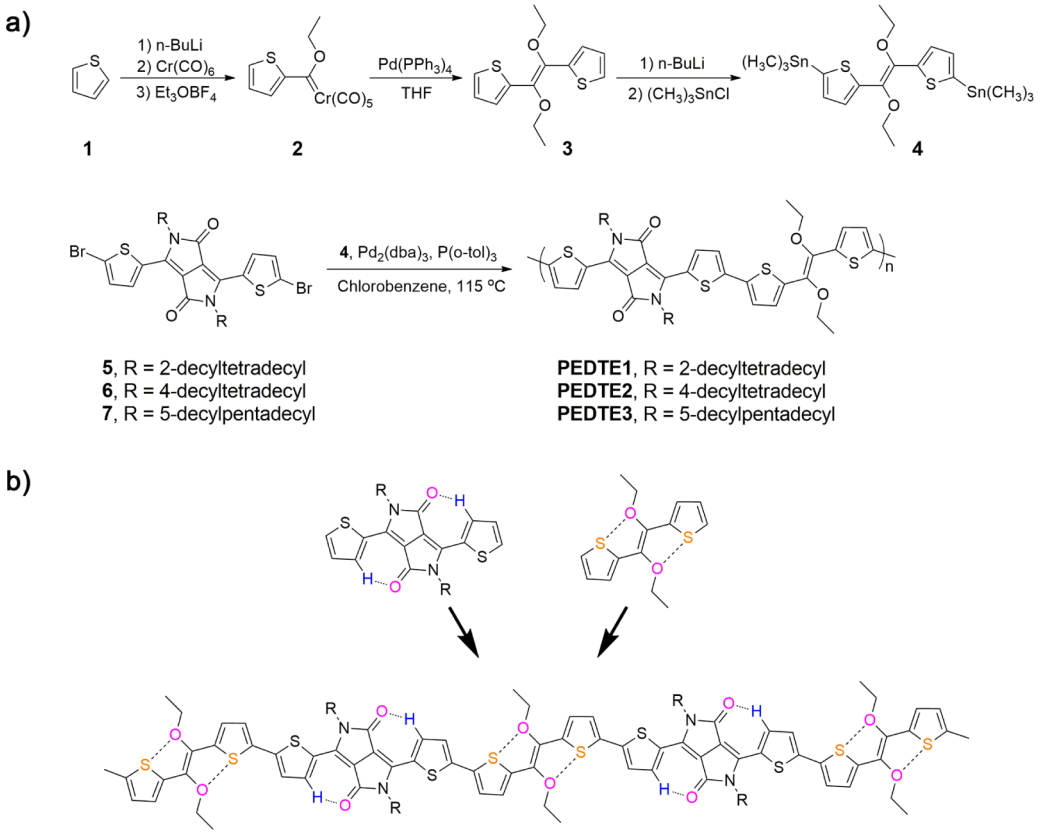

intramolecular S···O interactions (S−O distance of 3.03 Å predicted, the sum of van der Waals radii is 3.32 Å).[41] In the same year, Zhu and co-workers further analyzed the single crystal structures of cyano-functionalized dithienyl−DPP-based small molecules, indicating that the dithienyl−DPP-based small molecule assumes a significantly planar configuration with a very small dihedral angle of 7.74° between thiophene and DPP units due to the presence of intramolecular H bonds (C−H···O, 2.167 Å).[42] These deep investigations show that the noncovalent interactions are beneficial for obtaining planar conjugated backbone conformations, resulting in high charge carrier transport properties as aforementioned.

Inspired by the achievements, several noncovalent interactions have been purposefully introduced to polymeric skeletons and act as "conformational locks" to limit the free rotation of aromatic rings and to supply additional intermolecular interactions. In 2012, Facchetti and Marks et al. first synthesized diethoxydithiophenethene- (EDTE-) based small molecules and polymers, and put forward the concept of "conformational locks" on the basis of single crystal XRD data of EDTE. Among the EDTE-based materials containing S···O conformational locks, naphthalenediimide-*alt*-EDTE-based alternating polymer, P3 afforded a promising electron mobility of 0.5 $cm^2 V^{-1} s^{-1}$.[43] In the next few years, Pei and Yum et al. reported series of D−A copolymers containing several kinds of conformational locks. Their results indicated that both the incorporating positions and types of conformational locks have great influences on conjugated backbone conformations, leading to different charge carrier transport.[44,45] Our research group also developed series of D−A copolymers containing conformational locks and found that different fluorination positions could induce different types of conformational locks, thus resulting in different device performances.[46−48] Meanwhile, Jackson and co-workers assessed several kinds of nonbonding interactions by theoretical modeling, and gave their binding energy and equilibrium distances in a sequence of C−H···N, C−H···O, C−H···F, C−H···S, S···S, O···S, N···S, and F···S, in which F···S nonbonding interaction was thought to have the least potential for being used as potential "locking" mechanisms in small molecules and polymers.[49] To be frankly, however, substantially high-performance copolymers constructed based on the concept of conformational lock are rare to date.

In this work, we report a series of EDTE-based copolymers, namely PEDTE*n* (*n* = 1, 2, and 3) (Scheme 1). DETE and thiophene-flanked DPP units endow the resulting polymers with multiple intra- and intermolecular noncovalent interactions, including O···H−C and S···O conformational locks, which were confirmed by quantitative X−ray diffraction and computational results.[42,43] The copolymers show enhanced solution processability, broad absorption behaviors in UV−vis−NIR region both in solutions and thin films, and narrow optical bandgap of about 1.37 eV. Because the ethoxyl groups locate at the C═C linkage of EDTE moieties, all copolymers have low-lying HOMO energy levels of ca. −5.20 eV, which is of great necessity for acquiring high stable electronic devices. PFETs with bottom-gate/bottom-contact (BGBC) configuration based on these copolymers demonstrated typical p-type transport characteristics. The mobility of PEDTE*n* (*n* = 1, 2, and 3) shows an increasing trend with the extension of alkyl chain and the branching point of alkyl chains moving from π-conjugated backbones. Significantly, PEDTE3-based devices afford a high

DOI: 10.1021/acs.macromol.6b01510
Macromolecules XXXX, XXX, XXX−XXX

mobility of up to 5.37 $cm^2 V^{-1} s^{-1}$, which is among the highest mobility values obtained from D−A copolymers constructed based on the concept of conformational locks. Tapping-mode atomic force microscopy (AFM) and grazing incidence X-ray diffraction (GIXRD) analyses indicate that the PEDTE1 thin film owns highly ordered molecular packing and crystalline microstructure. With the alkylated side chains extending, however, the other copolymers adopt slightly random molecular packing mode in solid states.

EXPERIMENTAL SECTION

General Procedures and Requirements. The chemicals of $Cr(CO)_6$, $(Et_3O)BF_4$, *n*-BuLi, and Me_3SnCl were obtained from Acros. The catalysts of $Pd(PPh_3)_4$, $Pd_2(dba)_3$, and $P(o\text{-tol})_3$ were purchased from Sigma-Aldrich Chemicals. Tetrahydrofuran (THF) and hexane were freshly distilled over sodium wire/benzophenone under nitrogen before use. Dichloromethane was distilled over CaH_2. Other chemicals and solvents were used as received from commercial sources without further purification. (*E*)-1,2-Diethoxy-1,2-di(thiophen-2-yl)ethene (**3**), (*E*)-1,2-diethoxy-1,2-bis(5-(trimethylstannyl)thiophen-2-yl)ethene (**4**), and dibromodithienyl DPPs **5**, **6**, and **7** were prepared according to a previously established method.[43,46,50] All reactions were carried out using the Schlenk technique in inert atmosphere.

Measurements and Characterization. ^1H NMR and ^{13}C NMR spectra were recorded using a Bruker-300 NMR spectrometer referenced to the residual $CHCl_3$ 7.26 or $CDCl_3$ 77 ppm. High resolution mass spectrometry (HRMS) were collected on a Bruker APEXII or 9.4T Solarix FT-ICR mass spectrometers. Elemental analyses were carried on a CARLO ERBA 1106 elemental analyzer. Gel permeation chromatography (GPC) analyses were performed on a Polymer Laboratories PL 220 system using a refractive index detector at 150 °C, using 1,2,4-trichlorobenzene as an eluent with polystyrenes as standards. The UV−vis−NIR absorption spectra of all polymers were recorded on a Hitachi U-3010 spectrophotometer. The film absorption measurement samples were prepared by spin-coating polymer solution in chloroform onto quartz glass. Thermogravimetric analysis (TGA) measurements were carried out on a Perkin−Elmer series 7 thermal analysis system under N_2 at a heating rate of 10 °C min^{-1}. Cyclic voltammetry (CV) curves were collected on an electrochemistry workstation (CHI660A, Chenhua Shanghai) with a conventional three-electrode configuration in dry acetonitrile containing 0.1 M $n\text{-}Bu_4NPF_6$ using a platinum stick electrode, Ag/AgCl electrode, and platinum wire as working electrode, reference electrode, and counter electrode, respectively. The measurements were performed in a scan rate of 50 mV s^{-1} at room temperature. Surface morphology of polymer films was analyzed in air using a Digital Instruments Nanoscope V atomic force microscope operated in a tapping mode. The thin film samples were identical to those used in FET performance analysis. For 2D GIXRD, the drop-coated films were illuminated at a constant incidence angle of 0.2° ($\lambda = 2d \sin\theta = 1.24$ Å).

*$(C_4H_3S)C(OEt)[Cr(CO)_5]$ (**2**).* To a solution of thiophene (0.99 mL, 12.4 mmol) in 40 mL of dry THF was added dropwise 2.5 M *n*-BuLi in hexane (5.0 mL, 12.5 mmol) at −78 °C. The resulting solution was stirred for 1 h at the temperature. After the mixture being warmed to −40 °C, 2.5 g (11.4 mmol) of $Cr(CO)_6$ was gradually added under vigorous stirring. Then, the mixture was allowed to room temperature, and stirred for a further 15 min. After the reaction had been completed, solvents were removed under reduced pressure, the residue was washed with cold hexane, and the solid residual was dissolved in 40 mL of dichloromethane. $(Et_3O)BF_4$, in a 1.0 M solution in methylene chloride (12.4 mL, 12.4 mmol), was carefully added to the stirred mixture at −30 °C. Volatile materials were removed under reduced pressure. The solid residue was dissolved in 50 mL of dichloromethane, adsorbed onto cold silica gel, and then purified by silica gel column chromatography with petroleum ether/dichloromethane as eluent affording the desired product as a purple crystal (1.7 g, 43%). The product was directly used in the next reaction step without further purification.

*(E)-1,2-Diethoxy-1,2-di(thiophen-2-yl)ethene (**3**).* An established method was adopted using $(C_4H_3S)C(OEt)[Cr(CO)_5]$, **2** (1.54 g, 4.6 mmol), $Pd(PPh_3)_4$ (600 mg, 0.6 mmol), and anhydrous THF (60 mL) to give the title compound as a colorless crystalline solid (605 mg, 91%). ^1H NMR (300 MHz, $CDCl_3$, δ): 7.35−7.32 (m, 4H), 7.09 (dd, J = 4.8 Hz, J = 3.9 Hz, 2H), 3.89 (q, 4H), 1.45 (t, 6H). ^{13}C NMR (75 MHz, $CDCl_3$, δ): 140.4, 136.2, 126.5, 67.5, 15.5. HRMS: calcd for $[C_{14}H_{16}O_2S_2]^+$, 280.0592; found, 280.0595.

*(E)-1,2-Diethoxy-1,2-bis(5-(trimethylstannyl)thiophen-2-yl)ethene (**4**).* An established method was adopted using (*E*)-1,2-diethoxy-1,2-di(thiophen-2-yl)ethene, **3** (540 mg, 2.0 mmol), anhydrous THF (50 mL) 2.5 M solution of *n*-BuLi in hexane (2.0 mL, 5.0 mmol), and a 1.0 M solution of Me_3SnCl in THF (5.0 mL, 5.0 mmol) to afford the desired intermediate as a colorless crystal (860 mg, 72%). ^1H NMR (300 MHz, $CDCl_3$, δ): 7.44 (dd, J = 2.7 Hz, J = 0.9 Hz, 2H), 7.44 (dd, J = 3.3 Hz, J = 0.9 Hz, 2H), 3.91 (q, 4H), 1.46 (t, 6H), 0.39 (s, 18H). ^{13}C NMR (75 MHz, $CDCl_3$, δ): 142.2, 140.5, 139.4, 134.6, 126.4, 67.5, 15.5, −8.3. EI−MS: calcd for $[C_{20}H_{32}O_2S_2Sn_2]^+$, 607.9888; found, 607.9884.

General Synthetic Procedure of Copolymers PEDTE*n*. A Schlenk flask containing (*E*)-1,2-diethoxy-1,2-bis(5-(trimethylstannyl)-thiophen-2-yl)ethene, **4** (0.20 mmol), dibromodithienyl DPPs **5**, **6** or **7** (0.20 mmol), $Pd_2(dba)_3$ (9.0 mg), $P(o\text{-tol})_3$ (24.6 mg), and chlorobenzene (5.0 mL) was purged with Ar for 30 min at −78 °C, then heated to 115 °C and stirred for 24 h under Ar. After cooled to r.t., the resulting solution was precipitated in 200 mL of methanol containing 5 mL of HCl (aq.), and stirred for 3 h. The resulting polymer solid was filtered and subjected to Soxhlet extraction in methanol, acetone, and hexane for 24 h, respectively, for the residual catalytic metal and low-molecular-weight oligomers. The polymer residue was extracted with *o*-dichlorobenzene and precipitated in methanol, filtered, and dried under vacuum affording the desired polymers.

PEDTE1 (235 mg, 94%). ^1H NMR (300 MHz, d_4-$C_6D_4Cl_2$, δ): 9.23 (br, 2H), 7.42 (br, 4H), 7.20 (br, 2H), 4.31 (br, 4H), 4.10 (br, 4H), 2.34 (br, 4H), 1.63−1.28 (br, 74H), 1.00 (br, 12H). GPC: M_n = 63.4 kDa, M_w = 127.4 kDa, PDI = 2.01. Anal. Calcd for $C_{76}H_{118}N_2O_4S_4$: C, 72.91; H, 9.50; N, 2.24. Found: C 73.03, H 9.17, N 2.30.

PEDTE2 (230 mg, 92%). ^1H NMR (300 MHz, d_4-$C_6D_4Cl_2$, δ): 9.21 (br, 2H), 7.43 (br, 4H), 7.21 (br, 2H), 4.34 (br, 4H), 4.11 (br, 4H), 2.09 (br, 4H), 1.61−1.28 (br, 74H), 1.00 (br, 12H). GPC: M_n = 57.6 kDa, M_w = 119.8 kDa, PDI = 2.08. Anal. Calcd for $C_{76}H_{118}N_2O_4S_4$: C, 72.91; H, 9.50; N, 2.24. Found: C 71.30, H 9.21, N 2.29.

PEDTE3 (232 mg, 91%). ^1H NMR (300 MHz, d_4-$C_6D_4Cl_2$, δ): 9.21 (br, 2H), 7.45 (br, 4H), 7.20 (br, 2H), 4.36 (br, 4H), 4.11 (br, 4H), 2.06 (br, 4H), 1.72−1.28 (br, 78H), 1.00 (br, 12H). GPC: M_n = 57.3 kDa, M_w = 122.3 kDa, PDI = 2.13. Anal. Calcd for $C_{78}H_{122}N_2O_4S_4$: C, 73.19; H, 9.61; N, 2.19. Found: C 73.05, H 9.21, N 2.32.

General Procedures for PFETs Fabrication and Measurements. The BGBC PFET devices were fabricated using n^{2+}-Si/SiO_2 (300 nm) substrates, where n^{2+}-Si and SiO_2 were used as the gate electrode and gate dielectric, respectively. The source and drain gold electrodes were prepared by photolithography. The silica substrates were cleaned by using sonication in acetone, deionized water, ethanol, and then treated with octadecyltrichlorosilane (OTS), after which an OTS self-assembled monolayer formed on the gate dielectrics. Thin films (ca. 30 nm) of the polymer were deposited on the OTS-treated substrate by spin-coating using a polymer solution (10 mg/mL) in *o*-dichlorobenzene, prepared by dissolving the polymer in *o*-dichlorobenzene and stirring at 120 °C for 30 min. The optimal rotation speed is 2000 rpm. The as-spun thin films were optionally thermal annealed at 180 °C for 5 min on a hot plate in ambient condition. A Keithley 4200 SCS semiconductor parameter analyzer on a probe stage was employed to evaluate device performance in ambient condition. The charge carrier mobility in saturation (μ) was calculated from the following equation:

$$I_{DS} = (W/2L)C_i\mu(V_{GS} - V_{th})^2$$

DOI: 10.1021/acs.macromol.6b01510
Macromolecules XXXX, XXX, XXX−XXX

Table 1. Molecular Weight, Thermal, Optical and Electrochemical Properties of PEDTE*n*

copolymer	M_n (kDa)[a]	M_w (kDa)[a]	PDI[a]	T_{dec}[b] (°C)	λ_{max} (nm)	E_g^{opt} (eV)[e]	E_{onset}^{ox} (V)[f]	HOMO (eV)[f]	LUMO (eV)[g]
PEDTE1	63.4	127.4	2.00	326	744[c]/688, 749[d]	1.37	0.80	−5.20	−3.84
PEDTE2	57.6	119.8	2.08	328	751[c]/698, 756[d]	1.37	0.78	−5.18	−3.83
PEDTE3	57.2	122.3	2.13	350	755[c]/712, 759[d]	1.37	0.80	−5.20	−3.85

[a]Determined by GPC at 150 °C. [b]Onset decomposition temperature (5% weight loss) measured by TGA. [c]In chlorobenzene solutions. [d]In thin films. [e]Calculated from thin-film absorption edges (E_g^{opt} = 1240/$\lambda_{abs,onset}$). [f]Determined by CV. HOMO = −(4.4 + E_{onset}^{ox}) eV. [g]LUMO = (HOMO + E_g^{opt}) eV.

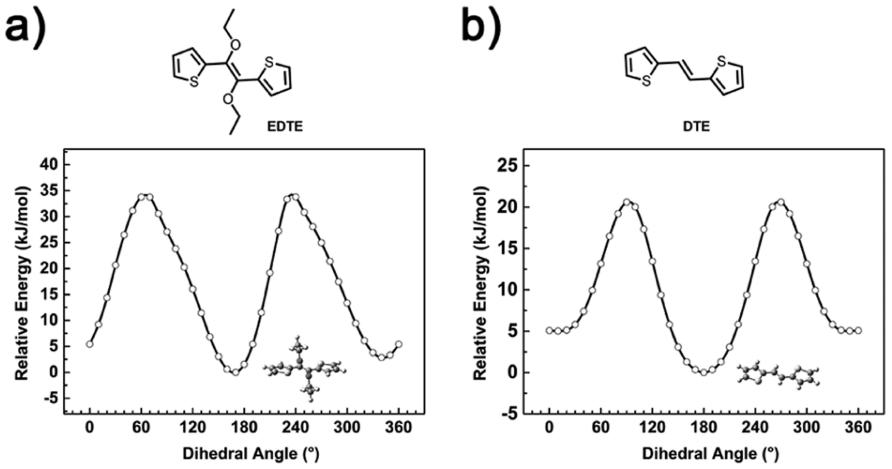

Figure 1. Gas-phase torsional potential energy distribution of EDTE and DTE units.

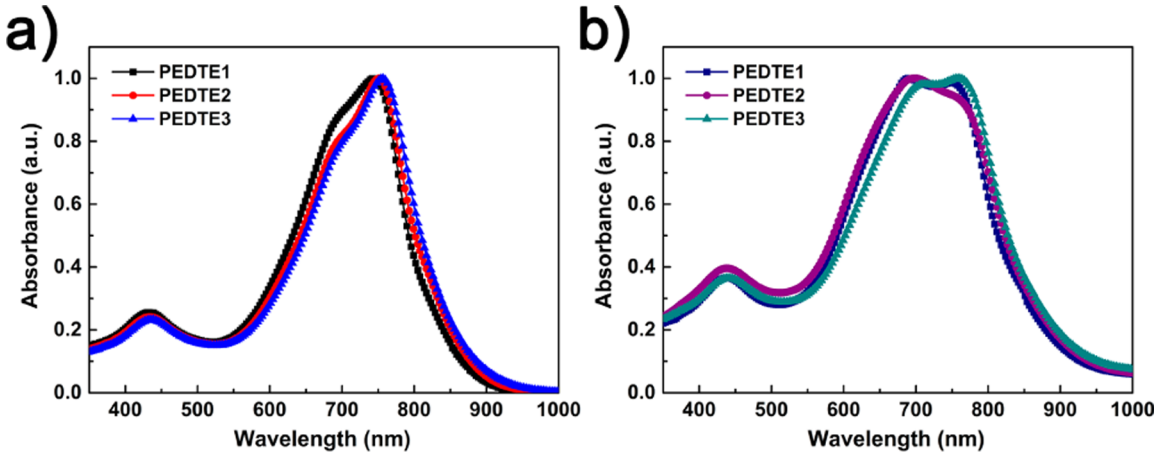

Figure 2. UV−vis−NIR absorption spectra of PEDTE*n* in (a) chlorobenzene and (b) thin films.

where W/L is the channel width/length, C_i is the gate dielectric layer capacitance per unit area, and V_{GS} and V_{th} are the gate voltage and threshold voltage, respectively. The channel lengths (L) and channel width (W) of the FET devices in our study are 50 and 1400 μm, respectively.

RESULTS AND DISCUSSION

Synthesis and Thermal Stability. The chemical structures and synthetic routes of PEDTE*n* (n = 1, 2, and 3) are shown in Scheme 1. The conversion from thiophene, **1**, to (*E*)-1,2-diethoxy-1′,2′-di(thiophen-2-yl)ethene, **3**, involving the thienylene−chromium carbene complex, **2**, which was synthesized according to the reported method of thienylene bridged binuclear biscarbene complex.[43,50] Thiophene reacted with *n*-BuLi, and followed by $Cr(CO)_6$ and $(Et_3O)BF_4$ at low temperature affording **2** as a purple crystal in a 43% yield.[50] In the presence of $Pd(PPh_3)_4$, **2** was converted to the desired intermediate **3** in a 91% yield.[43] Then, a tin intermediate **4** was synthesized as a colorless crystal according to a reported method.[43] Stille-coupling polymerization between 2-decyltetradecyl, 4-decyltetradecyl, or 5-decylpentadecyl-substituted dibromo-dithienyl DPPs, **5**, **6**, and **7**, which were synthesized according to previous literature,[46] with intermediate **4** gave the crude copolymers. After purification of the precipitation into methanol and the removal of low-molecular-weight and catalytic impurities of the resultant polymer by Sohxlet extraction were afforded the title polymer materials in high yields, respectively. PEDTE*n* (n = 1, 2, and 3) has good solubility in chlorinated solvents, such as chlorobenzene, *o*-dichlorobenzene, and so forth. The copolymers were characterized by high temperature ^{1}H NMR and GPC. The number-average molecular weight (M_n) and the polydispersity indexes (PDIs) were found to be 63.4 kDa and 2.00 for PEDTE1, 57.6 kDa and 2.08 for PEDTE2, and 57.2 kDa and

DOI: 10.1021/acs.macromol.6b01510
Macromolecules XXXX, XXX, XXX−XXX

2.13 for PEDTE3, respectively (Table 1). Thermal properties of PEDTE*n* (n = 1, 2, and 3) were also evaluated by TGA and differential scanning calorimetry (DSC). The decomposition temperatures (T_{dec}) with 5% weight loss for the three polymers are 326, 328, and 350 °C, respectively (Figure S1, Supporting Information). No apparent phase transition was observed in DSC traces of the three copolymers in the range of 50 to 250 °C.

Theoretical Modeling of EDTE Unit. As noticed above, Facchetti and Marks et al. have prepared the single crystal of EDTE for XRD. Its planarity is evident in the single crystal. The S···O interactions have also been indicated by XRD analysis. To obtain more sight of EDTE unit, we calculated the torsional potentials. We performed a gas-phase dihedral potential energy scan (Figure 1). Relaxed potential energy scans were carried out for thiophene-diethoxyvinylthiophene subunits at 10° intervals. The dihedral angle was constrained (0−360°, altogether 37 conformational isomers) and all other degrees of freedom were allowed to relax to their energy minima at the B3LYP/6-31G* level.[51] There are nonbonding interactions in these systems, which make the conventional DFT methods unreliable to obtain accurate energies. Therefore, single point energies were further calculated at mp2/cc-pvdz level (Figure 1a). Two local conformational energy minima were found at 170° and 340°. The dihedral barrier is about 33.8 kJ/mol. In order to better clarify the effect of S···O interaction, a similar calculation was also performed for the (*E*)-1,2-di(thiophen-2-yl)ethene (DTE) unit. The DTE unit also has two local conformational energy minima located at 0° and 180°, and its dihedral barrier is about 20.6 kJ/mol (Figure 2b). The calculation results indicate that EDTE unit has higher torsional potential than that of DTE unit. In other words, the ethoxyl groups endow EDTE unit with the S···O interactions, which could effectively limit the free rotation of conjugated backbone. To obtain more information, we also calculated one repeat unit of EDTE-based copolymers and further investigated the electronic structures by comparing with the unsubstituted DTE counterpart. The results reveal the existence of small dihedral angles of 7.0° and 11.8° in the DPP−EDTE subunit, meaning that there is a slight distortion in DPP−EDTE compared to DPP−DTE (Figure S2).

Optical Properties. The optical properties of PEDTE*n* in solutions and thin films were studied by absorption spectroscopy (Figure 2). In chlorobenzene solutions, PEDTE*n* (n = 1, 2, and 3) exhibits broad absorption profiles in the UV−vis−NIR zone (Figure 2a). The high-energy absorption bands of 300−500 nm is corresponding to π−π^* transition of the conjugated backbone. The low-energy absorption bands ranging from 550 to ca. 900 nm are attributed to intramolecular charge transfer between donor and acceptor units.[25] With the change of alkyl chains and branching point of alkyl chains moving from π-conjugated backbones, the resulting polymers, PEDTE*n*, show slightly red-shifted absorption behaviors, hinting that PEDTE3 owns more planar conjugated backbone than the other two copolymers due to less steric repulsion between side chains.[52] Compared to the ones in solutions, thin films of PEDTE*n* (n = 1, 2, and 3) display broader absorption spectra. PEDTE1 and PEDTE2 exhibit a blue-shift in absorption spectra (~50 nm), whereas PEDTE3 exhibits a slight red-shift (~4 nm). For PEDTE1 and PEDTE2, the blue-shifts are due to aggregation that amplifies the vibronic signals (and relative intensities). For PEDTE3, however, the red-shift could be attributed to the fact that the impact of alkyl chains on the aggregation is weaker. The observations demonstrate that the three alkyl side chains exert different influences on the interchain interactions, π−π stacking, and conjugated backbone planarity of the PEDTE*n* in solid state. In addition, on the basis of absorption edges (~900 nm), the optical band gaps of PEDTE*n* (n = 1, 2, and 3) were estimated to be ~1.37 eV.

Electrochemical Properties. CV traces of the PEDTE*n* thin films spin-coated onto a platinum stick working electrode are displayed in Figure S3. The three copolymers show strong and almost the same onset oxidation potentials at around 0.80 V, based on which the HOMO energy levels of PEDTE*n* (n = 1, 2, and 3) were estimated to be ca. − 5.20 eV, calculated from the equation of HOMO = $-(4.4 + E_{onset}^{ox})$ eV.[45] The HOMO energy levels are slightly higher (~0.10 eV) than −5.30 eV of the copolymers, poly{3,6-dithien-2-yl-2,5-di(2-alkyl)-pyrrolo[3,4-*c*]pyrrole-1,4-dione-5′,5″-diyl-*co*-(*E*)-1,2-di(thiophen-2-yl)-ethene-5,5′-diyl} (PDVT).[20] The difference is apparently lower than 0.20 eV of between those of copolymers poly{3,6-dithien-2-yl-2,5-di(2-alkyl)-pyrrolo[3,4-*c*]pyrrole-1,4-dione-5′,5″-diyl-*co*-3,6-dimethoxythieno[3,2-*b*]thiophene-2,5′-diyl} (PDMOTT, − 5.02 eV) and poly{3,6-dithien-2-yl-2,5-di(2-alkyl)-pyrrolo[3,4-*c*]pyrrole-1,4-dione-5′,5″-diyl-*co*-thieno[3,2-*b*]thiophene-2,5′-diyl} (PDBT-*co*-TT, − 5.25 eV).[46,53] The results show that two ethoxyl groups located at the C═C linkage have less destabilizing impact on the HOMOs, as Facchetti and Marks et al. pointed out.[43] Unfortunately, no ideal reduction curve was obtained for the three copolymers by the CV method after several attempts. Thus, the LUMO energy levels were estimated to be ca. −3.85 eV from the differences between the HOMO energy levels and optical bandgaps. In an attempt to further predict the optoelectronic properties of the EDTE-based copolymers, a molecular modeling of polymer planarity and HOMO/LUMO distribution were performed using DFT/B3LYP method with a B3LYP/6-31G* basis set. Calculation results reveal that PEDTE*n* also possesses almost planar conjugated backbone (optimized angles, 1.4 and 12.5°), and their HOMOs and LUMOs are well-delocalized along polymer backbones (Figure 3). The results agree with the optimized structures of one repeat unit as shown in Figure S2.

Field-Effect Transistor Fabrication and Measurements. PFETs with the BGBC configuration were fabricated to investigate the charge carrier transport properties of the three copolymers. The fabrication details of the devices are included in the experimental section. Besides fabrication,

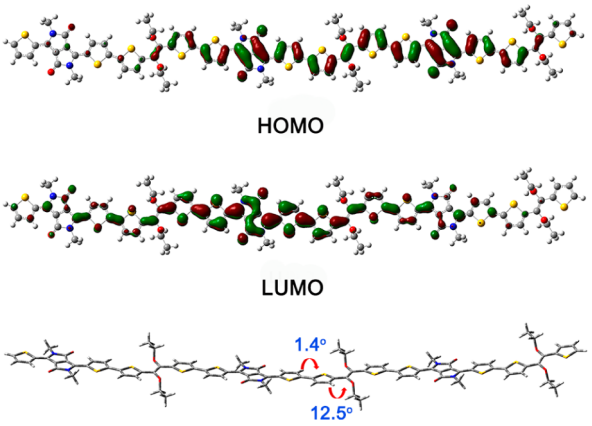

Figure 3. Optimized molecular structure and molecular frontier orbitals of the PEDTE*n* (trimer) (B3LYP/6-31G*).

DOI: 10.1021/acs.macromol.6b01510
Macromolecules XXXX, XXX, XXX−XXX

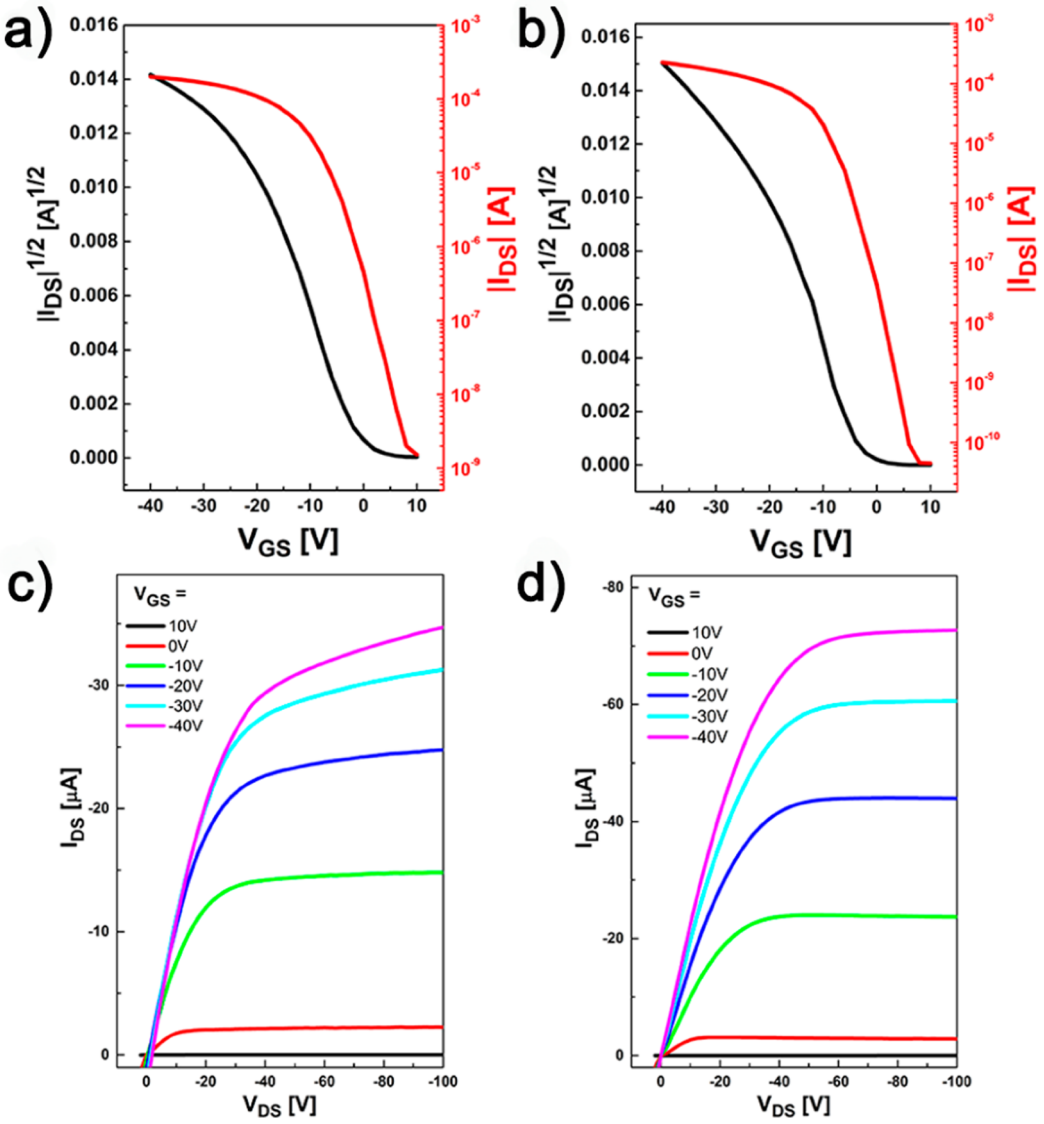

Figure 4. Typical transfer and output characteristics (V_{DS} = −100 V) of PFETs based on (a, c) PEDTE2 and (b, d) PEDTE3 after annealing at an optimal temperature of 180 °C.

Table 2. Device Performance of the PEDTE*n*-Based PFETs

copolymer	temperature (°C)	μ^b (μ_{max}) (cm^2 V^{-1} s^{-1})	$I_{on}/I_{off}{}^b$	$V_{th}{}^b$ (V)	$\pi-\pi^c$ (Å)	d−d^c (Å)
PEDTE1	as-spun	0.07 ± 0.01 (0.10)	10^3−10^4	0 to 4		
	180[a]	1.49 ± 0.22 (2.07)	10^5−10^6	0 to 4	3.89	22.5
PEDTE2	as-spun	0.09 ± 0.01 (0.13)	10^4−10^5	−2 to +2		
	180[a]	2.75 ± 0.21 (3.48)	10^5−10^6	−5 to +2	3.78	23.1
PEDTE3	as-spun	0.11 ± 0.01 (0.15)	10^4−10^5	−3 to +3		
	180[a]	4.38 ± 0.35 (5.37)	10^5−10^6	−5 to +2	3.78	24.0

[a]Optimal annealing temperature. [b]Mobility, on/off ratio, and threshold voltage were summarized from more than 20 devices. [c]The distances of $\pi-\pi$ and d− stacking in thin films.

subsequent annealing and testing process were all performed under ambient conditions. The typical output ($I_{DS} - V_{DS}$) and transfer ($I_{DS} - V_{GS}$) plots are presented in Figures 4 and S4, and the extracted electrical parameters of the PFETs are listed in Table 2. The average field-effect mobilities were calculated from the transfer characteristics of more than 20 devices in the saturation region (V_{DS} = −100 V). As anticipated, the PFETs based on PEDTE*n* (*n* = 1, 2, and 3) all show p-type transport characteristics.

After being annealed at an optimal temperature of 180 °C for 5 min, the PFETs exhibited high saturation mobility of 1.49 ± 0.22 cm^2 V^{-1} s^{-1} for PEDTE1, 2.75 ± 0.21 cm^2 V^{-1} s^{-1} for PEDTE2, and 4.38 ± 0.35 cm^2 V^{-1} s^{-1} for PEDTE3, respectively, with on/off current ratios of 10^5−10^6. The maximum mobility of the PEDTE3-based devices was determined to be as high as 5.37 cm^2 V^{-1} s^{-1}, which is among the highest values of polymers constructed based on the concept of conformational locks to our knowledge. With the

DOI: 10.1021/acs.macromol.6b01510
Macromolecules XXXX, XXX, XXX−XXX

extension of alkyl side chain and the branching point moving away from backbone, the hole mobility of PEDTE*n* increased significantly, and the change trend is consistent with other polymer semiconductors in previous works.[53] The enhanced mobility of PEDTE3 can be attributed to its more exposed conjugated core, leading to a closer molecular packing and stronger $\pi-\pi$ interaction in thin films. In nature, the shorter alkyl side chains of PEDTE1 and PEDTE2 play larger effect on entropically penalizing aggregate formation by interrupting $\pi-\pi$ interactions between polymer chains than that of PEDTE3 with longer alkyl side chains.[54] The differences have been demonstrated by their UV−vis−NIR spectra of the three copolymers as aforementioned. The annealing temperature-dependent mobilities of the PEDTE*n*-based devices are collected in Table S1. The as-spun films of PEDTE*n* only afford lower mobilities of 0.10−0.15 $cm^2\ V^{-1}\ s^{-1}$ along with lower on/off current ratios. With the increasing of annealing temperatures, the mobilities of all copolymers also improved. Nevertheless, when annealing temperature rises to 200 °C, the mobilities of all copolymers decrease in different degrees. These observations imply that thermal-induced molecular self-assembly occurred in the annealing process.

Thin Film Microstructural Characterization. To understand the correlation between thin film microstructures and transistor performances, tapping-mode AFM and GIXRD technique were adopted to investigate the thin-film samples deposited on OTS-modified SiO_2 substrates. Figures S5 and 5 exhibit the AFM images of PEDTE*n* as-spun thin films and thin films after being thermally annealed at 180 °C for 5 min under ambient conditions. The annealed PEDTE1 thin film exhibits fiber-like intercalating networks with obviously enlarged crystalline zones in comparison with the as-spun one. The large crystalline grains are thought to be beneficial for charge carrier transport, whereas slightly deep grain boundaries may result in trapping of charge carriers. With the extension of alkyl side chains, the PEDTE*n* thin films show a trend of polymer fibers becoming smaller and grain boundaries becoming fewer. Eventually, the PEDTE3 thin film presents a highly uniform and dense morphology with fiber-like intercalating network, which is attributed to the enhanced intermolecular $\pi-\pi$ interactions and is more beneficial for charge carrier transport as demonstrated in several high-performance polymer semiconductors.

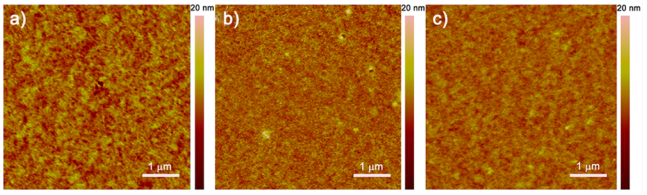

Figure 5. AFM topography images of the PEDTE*n* thin films annealed at 180 °C for 5 min on OTS-modified SiO_2/Si substrates: (a) PEDTE1, (b) PEDTE2, and (c) PEDTE3. AFM images are 5 μm × 5 μm in size.

Figures S6 and 6 show the 2D-GIXRD images of PEDTE*n* as-spun thin films and annealed thin films, respectively. GIXRD images demonstrate that the annealed thin films own distinctly enhanced diffraction peaks in comparison with their respective as-spun thin films, implying that the annealed thin films have more ordered molecular aggregation. The relevant crystallographic parameters are summarized in Table 2. PEDTE1 has a highly ordered, lamellar crystalline structure as judged from the presence of the (h00) Bragg diffraction peaks in out-of-plane (q_z) orientation, in which strong (100), (200), (300), and even (400) Bragg diffraction peaks could be observed in the annealed thin films. On the contrary, PEDTE2 and PEDTE3 exhibit fewer diffraction peaks, and these peaks are remarkably broad, implying that the two copolymers have low-ordered structures. On the basis of the Bragg peak of (100) at q_z of 3.16, 3.08, and 2.96 nm^{-1}, the d−d spacing distance was estimated to be 22.5 Å for PEDTE1, 23.1 Å for PEDTE2, and 24.0 Å for PEDTE3, respectively. The (010) Bragg diffraction peak assigned to be $\pi-\pi$ stacking was also observed in their respective in-plane (q_{xy}) patterns. For PEDTE1, no (010) Bragg peak was found in out-of-plane (q_z) pattern, suggesting that the copolymer takes an edge-on molecular packing orientation to (OTS)-modified Si/SiO_2 substrate in thin films. For PEDTE2 and PEDTE3, however, their (010) Bragg peaks are semicircle, and appear in both q_{xy} and q_z orientations. The observations indicate that the two copolymers own comparatively random close packing modes in solid states, resulting from the longer alkyl side chains. The $\pi-\pi$ stacking distances of PEDTE*n* (n = 1, 2, and 3) were estimated to be 3.89, 3.78, and 3.78 Å on the basis of the q_{xy} of 22.8, 23.5, and 23.5 nm^{-1}, respectively. There are larger differences among the GIXRD patterns of the three copolymers for their as-spun thin films and after annealed ones. It could be attributed to the fact that molecular aggregations or $\pi-\pi$ stacking pattern of polymer materials are heavy affected by thermal annealing process besides the chemical structure of polymer materials.[55] Upon a systematic optimization on thermal annealing conditions, the annealed polymer thin films may exhibit a completely different molecular aggregations to its as-spun counterparts. Generally speaking, these AFM and GIXRD images are helpful to explain

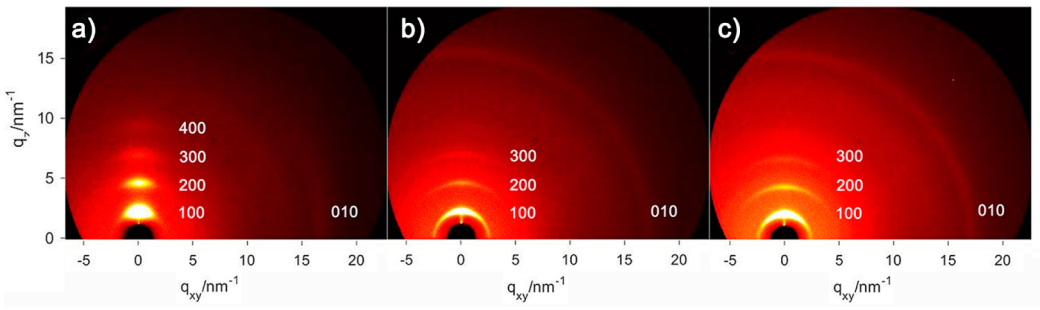

Figure 6. 2D-GIXRD patterns of the PEDTE*n* thin films annealed at 180 °C for 5 min on OTS-modified SiO_2/Si substrates: (a) PEDTE1, (b) PEDTE2, and (c) PEDTE3.

DOI: 10.1021/acs.macromol.6b01510
Macromolecules XXXX, XXX, XXX−XXX

the mobility differences between the three copolymers: highly ordered molecular packing is indeed favorable for high charge mobilities, however, it is only true for charge transport within the crystalline grains. PEDTE1 has a lot of grain boundaries that hinder charge transport along long distances in contrast to PEDTE3 for which more molecules closely packed over small π-distances are connecting the small crystalline grains.

CONCLUSION

To sum up, we have synthesized and characterized a series of diethoxydithiophenethene (EDTE)-based copolymers, PEDTE*n* (n = 1, 2, and 3). The introduction of EDTE unit to DPP-based conjugated backbone endows the series of copolymers with multiple O···H−C and S···O conformational locks, inducing a highly planar backbone conformation and enhanced solution processability. The low-lying HOMO energy levels (−5.20 eV) of PEDTE*n* demonstrate the importance of conformational locks in functionalized sites. PFET devices based on PEDTE*n* exhibited high hole mobility of up to 5.37 $cm^2\ V^{-1}\ s^{-1}$ with on/off current ratios of $10^5 \sim 10^6$. These findings highlight the important meaning of conformational locks on tuning the optical, electrochemical, thermal properties, and intra- and intermolecular interactions of semiconducting copolymers.

ASSOCIATED CONTENT

Supporting Information

The Supporting Information is available free of charge on the ACS Publications website at DOI: 10.1021/acs.macromol.6b01510.

TGA traces, optimized structures of the DPP−EDTE and DPP−DTE repeat units, CV traces of PEDTE*n*, output and transfer plots of PEDTE1, mobility data, NMR spectra of EDTE-based intermediates **3** and **4** and the copolymers, and AFM and GIXRD images of the PEDTE*n* as-spun films (PDF)

AUTHOR INFORMATION

Corresponding Author

*E-mail: yugui@iccas.ac.cn (G.Y.).

Author Contributions

†W.Z. and Z.M. contributed equally to this work.

Notes

The authors declare no competing financial interest.

ACKNOWLEDGMENTS

This work was financially supported by the Strategic Priority Research Program of the Chinese Academy of Sciences (XDB12030100) and the National Natural Science Foundation of China (Grants 21474116 and 51233006), The GIXRD tests were carried out at the BL16B1 Station of Shanghai Synchrotron Radiation Facility (SSRF), 1W1A station of Beijing Synchrotron Radiation Facility (BSRF), and 23A1 Station of National Synchrotron Radiation Research Centre (NSRRC, Taiwan). The authors gratefully express thanks for the assistance of scientists from the stations during the experiments.

REFERENCES

(1) Venkateshvaran, D.; Nikolka, M.; Sadhanala, A.; Lemaur, V.; Zelazny, M.; Kepa, M.; Hurhangee, M.; Kronemeijer, A. J.; Pecunia, V.; Nasrallah, I.; Romanov, I.; Broch, K.; McCulloch, I.; Emin, D.; Olivier, Y.; Cornil, J.; Beljonne, D.; Sirringhaus, H. Approaching Disorder-Free Transport in High-Mobility Conjugated Polymers. *Nature* **2014**, *515*, 384−388.

(2) Wu, W. B.; Tang, R. L.; Li, Q. Q.; Li, Z. Functional Hyperbranched Polymers with Advanced Optical, Electrical and Magnetic Properties. *Chem. Soc. Rev.* **2015**, *44*, 3997−4022.

(3) Wang, L. P.; Xie, X. D.; Shi, S. W.; Shi, K. L.; Mao, Z. P.; Zhang, W. F.; Wang, H. Q.; Yu, G. Synthesis, Characterization, and Field-Effect Properties of (*E*)-2-(2-(Thiophen-2-yl)vinyl)thiophen-Based Donor-Acceptor Copolymers. *Polymer* **2015**, *68*, 302−307.

(4) He, Z. C.; Zhong, C. M.; Su, S. J.; Xu, M.; Wu, H. B.; Cao, Y. Enhanced Power-Conversion Efficiency in Polymer Solar Cells Using an Inverted Device Structure. *Nat. Photonics* **2012**, *6*, 591−595.

(5) You, J. B.; Dou, L. T.; Yoshimura, K.; Kato, T.; Ohya, K.; Moriarty, T.; Emery, K.; Chen, C.-C.; Gao, J.; Li, G.; Yang, Y. A. Polymer Tandem Solar Cell with 10.6% Power Conversion Efficiency. *Nat. Commun.* **2013**, *4*, 1446.

(6) Deng, Y. F.; Liu, J.; Wang, J. T.; Liu, L. H.; Li, W. L.; Tian, H. K.; Zhang, X. J.; Xie, Z. Y.; Geng, Y. H.; Wang, F. S. Dithienocarbazole and Isoindigo Based Amorphous Low Bandgap Conjugated Polymers for Efficient Polymer Solar Cells. *Adv. Mater.* **2014**, *26*, 471−476.

(7) Wang, E. G.; Ma, Z.; Zhang, Z.; Vandewal, K.; Henriksson, P.; Inganas, O.; Zhang, F.; Andersson, M. R. An Easily Accessible Isoindigo-Based Polymer for High-Performance Polymer Solar Cells. *J. Am. Chem. Soc.* **2011**, *133*, 14244−14247.

(8) Tan, Z. A.; Zhang, W. Q.; Zhang, Z. G.; Qian, D. P.; Huang, Y.; Hou, J. H.; Li, Y. F. High-Performance Inverted Polymer Solar Cells with Solution-Processed Titanium Chelate as Electron-Collecting Layer on ITO Electrode. *Adv. Mater.* **2012**, *24*, 1476−1481.

(9) Chen, J.-D.; Cui, C.; Li, Y.-Q.; Zhou, L.; Ou, Q.-D.; Li, C.; Li, Y.; Tang, J.-X. Single-Junction Polymer Solar Cells Exceeding 10% Power Conversion Efficiency. *Adv. Mater.* **2015**, *27*, 1035−1041.

(10) Sirringhaus, H. 25th Anniversary Article: Organic Field-Effect Transistors: The Path beyond Amorphous Silicon. *Adv. Mater.* **2014**, *26*, 1319−1335.

(11) Yan, H.; Chen, Z. H.; Zheng, Y.; Newman, C.; Quinn, J. R.; Dötz, F.; Kastler, M.; Facchetti, A. A High-Mobility Electron-Transporting Polymer for Printed Transistors. *Nature* **2009**, *457*, 679−686.

(12) Wang, C. L.; Dong, H. L.; Hu, W. P.; Liu, Y. Q.; Zhu, D. B. Semiconducting π-Conjugated Systems in Field-Effect Transistors: A Material Odyssey of Organic Electronics. *Chem. Rev.* **2012**, *112*, 2208−2267.

(13) Tsao, H. N.; Cho, D. M.; Park, I.; Hansen, M. R.; Mavrinskiy, A.; Yoon, D. Y.; Graf, R.; Pisula, W.; Spiess, H. W.; Müllen, K. Ultrahigh Mobility in Polymer Field-Effect Transistors by Design. *J. Am. Chem. Soc.* **2011**, *133*, 2605−2612.

(14) Zhang, W. F.; Liu, Y. Q.; Yu, G. Heteroatom Substituted Organic/Polymeric Semiconductors and their Applications in Field-Effect Transistors. *Adv. Mater.* **2014**, *26*, 6898−6904.

(15) Zhang, F. J.; Zang, Y. P.; Huang, D. Z.; Di, C. A.; Zhu, D. B. Flexible and Self-Powered Temperature-Pressure Dual-Parameter Sensors Using Microstructure-Frame-Supported Organic Thermoelectric Materials. *Nat. Commun.* **2015**, *6*, 8356.

(16) Crone, B.; Dodabalapur, A.; Lin, Y. Y.; Filas, R. W.; Bao, Z.; LaDuca, A.; Sarpeshkar, R.; Katz, H. E.; Li, W. Large-Scale Complementary Integrated Circuits Based on Organic Transistors. *Nature* **2000**, *403*, 521−523.

(17) Zang, Y. P.; Zhang, F. J.; Huang, D. Z.; Gao, X. K.; Di, C. A.; Zhu, D. B. Flexible Suspended Gate Organic Thin-Film Transistors for Ultra-Sensitive Pressure Detection. *Nat. Commun.* **2015**, *6*, 6269.

(18) Tee, B. C. K.; Wang, C.; Allen, R.; Bao, Z. An Electrically and Mechanically Self-Healing Composite with Pressure and Flexion-Sensitive Properties for Electronic Skin Applications. *Nat. Nanotechnol.* **2012**, *7*, 825−832.

(19) Kim, G.; Kang, S. J.; Dutta, G. K.; Han, Y. K.; Shin, T. J.; Noh, Y. Y.; Yang, C. A Thienoisoindigo−Naphthalene Polymer with Ultrahigh Mobility of 14.4 cm^2/Vs that Substantially Exceeds

DOI: 10.1021/acs.macromol.6b01510
Macromolecules XXXX, XXX, XXX−XXX

Benchmark Values for Amorphous Silicon Semiconductors. *J. Am. Chem. Soc.* **2014**, *136*, 9477−9483.
(20) Tseng, H. R.; Phan, H.; Luo, C.; Wang, M.; Perez, L. A.; Patel, S. N.; Ying, L.; Kramer, E. G.; Nguyen, T. Q.; Bazan, G. C.; Heeger, A. J. High-Mobility Field-Effect Transistors Fabricated with Macroscopic Aligned Semiconducting Polymers. *Adv. Mater.* **2014**, *26*, 2993−2998.
(21) Chen, H. J.; Guo, Y. L.; Yu, G.; Zhao, Y.; Zhang, J.; Gao, D.; Liu, H. T.; Liu, Y. Q. Highly π-Extended Copolymers with Diketopyrrolopyrrole Moieties for High-Performance Field-Effect Transistors. *Adv. Mater.* **2012**, *24*, 4618−4622.
(22) Kang, I.; Yun, H. J.; Chung, D. S.; Kwon, S. K.; Kim, Y. H. Record High Hole Mobility in Polymer Semiconductors via Side-Chain Engineering. *J. Am. Chem. Soc.* **2013**, *135*, 14896−14899.
(23) Li, J.; Zhao, Y.; Tan, H. S.; Guo, Y. L.; Di, C. A.; Yu, G.; Liu, Y. Q.; Lin, M.; Lim, S. H.; Zhou, Y. H.; Su, H. B.; Ong, B. S. A Stable Solution-Processed Polymer Semiconductor with Record High Mobility for Printed Transistors. *Sci. Rep.* **2012**, *2*, 754.
(24) Coughlin, J. E.; Zhugayevych, A.; Bakus, R. C., II; van der Poll, T. S.; Welch, D. C.; Teat, S. J.; Bazan, G. C.; Tretiak, S. A Combined Experimental and Theoretical Study of Conformational Preferences of Molecular Semiconductors. *J. Phys. Chem. C* **2014**, *118*, 15610−15623.
(25) Nketia-Yawson, B.; Lee, H. S.; Seo, D.; Yoon, Y.; Park, W. T.; Kwak, K.; Son, H. J.; Kim, B.; Noh, Y. Y. A Highly Planar Fluorinated Benzothiadiazole-Based Conjugated Polymer for High-Performance Organic Thin-Film Transistors. *Adv. Mater.* **2015**, *27*, 3045−3052.
(26) Lei, T.; Cao, Y.; Zhou, X.; Peng, Y.; Bian, J.; Pei, J. Systematic Investigation of Isoindigo-Based Polymeric Field-Effect Transistors: Design Strategy and Impact of Polymer Symmetry and Backbone Curvature. *Chem. Mater.* **2012**, *24*, 1762−1770.
(27) Yang, N.; Qiao, X. L.; Fang, R. R.; Tao, J. W.; Hao, J.; Li, H. X. Syntheses and Properties of Five-Ring Fused Azo- and Thio-Aromatic Compounds Containing Imide Substituent. *Huaxue Xuebao* **2016**, *74*, 335−339.
(28) Zhu, M. L.; Luo, H.; Wang, L. P.; Yu, G.; Liu, Y. Q. Synthesis of Pentacene Analogues Containing Heteroatoms and Study of their Field-Effect Performance. *Huaxue Xuebao* **2012**, *70*, 1599−1603.
(29) Ha, J. S.; Kim, K. H.; Choi, D. H. 2,5-Bis(2-octyldodecyl) pyrrolo[3,4-*c*]pyrrole-1,4-(2*H*,5*H*)-dione-Based Donor−Acceptor Alternating Copolymer Bearing 5,5′-Di(thiophen-2-yl)-2,2′-biselenophene Exhibiting 1.5 $cm^2\ V^{-1}\ s^{-1}$ Hole Mobility in Thin-Film Transistors. *J. Am. Chem. Soc.* **2011**, *133*, 10364−10367.
(30) Huang, J. Y.; Mao, Z. P.; Chen, Z. H.; Gao, D.; Wei, C. Y.; Zhang, W. F.; Yu, G. Diazaisoindigo Based Polymers with High-Performance Charge Transport Properties: From Computational Screening to Experimental Characterization. *Chem. Mater.* **2016**, *28*, 2209−2218.
(31) Chen, H. J.; Guo, Y. L.; Mao, Z. P.; Yu, G.; Huang, J. Y.; Zhao, Y.; Liu, Y. Q. Naphthalenediimide-Based Copolymers Incorporating Vinyl-Linkages for High-Performance Ambipolar Field-Effect Transistors and Complementary-like Inverters under Air. *Chem. Mater.* **2013**, *25*, 3589−3596.
(32) Lee, J.; Han, A. R.; Yu, H.; Shin, T.; Yang, C.; Oh, J. H. Boosting the Ambipolar Performance of Solution-Processable Polymer Semiconductors via Hybrid Side-Chain Engineering. *J. Am. Chem. Soc.* **2013**, *135*, 9540−9547.
(33) Kim, K.-H.; Park, S.; Yu, H.; Kang, H.; Song, I.; Oh, J. H.; Kim, B. J. Determining Optimal Crystallinity of Diketopyrrolopyrrole-Based Terpolymers for Highly Efficient Polymer Solar Cells and Transistors. *Chem. Mater.* **2014**, *26*, 6963−6970.
(34) Stalder, R.; Puniredd, S. R.; Hansen, M. R.; Koldemir, U.; Grand, C.; Zajaczkowski, W.; Müllen, K.; Pisula, W.; Reynolds, J. R. Ambipolar Charge Transport in Isoindigo-Based Donor−Acceptor Polymers. *Chem. Mater.* **2016**, *28*, 1286−1297.
(35) Zhou, X.; Ai, N.; Guo, Z. H.; Zhuang, F. D.; Jiang, Y. S.; Wang, J.-Y.; Pei, J. Balanced Ambipolar Organic Thin-Film Transistors Operated under Ambient Conditions: Role of the Donor Moiety in BDOPV-Based Conjugated Copolymers. *Chem. Mater.* **2015**, *27*, 1815−1820.
(36) An, C. B.; Li, M. M.; Marszalek, T.; Li, D.; Berger, R.; Pisula, W.; Baumgarten, M. Thiadizoloquinoxaline-Based Low-Bandgap Conjugated Polymers as Ambipolar Semiconductors for Organic Field Effect Transistors. *Chem. Mater.* **2014**, *26*, 5923−5929.
(37) Yi, Z. R.; Ma, L. C.; Chen, B.; Chen, D. G.; Chen, X. G.; Qin, J. G.; Zhan, X. W.; Liu, Y. Q.; Ong, W. J.; Li, J. Effect of the Longer β-Unsubstituted Oligothiophene Unit (6T and 7T) on the Organic Thin-Film Transistor Performances of Diketopyrrolopyrrole−Oligothiophene Copolymers. *Chem. Mater.* **2013**, *25*, 4290−4296.
(38) Li, Y. N.; Sonar, P.; Singh, S. P.; Soh, M. S.; van Meurs, M.; Tan, J. Annealing-Free High-Mobility Diketopyrrolopyrrole−Quaterthiophene Copolymer for Solution-Processed Organic Thin Film Transistors. *J. Am. Chem. Soc.* **2011**, *133*, 2198−2204.
(39) Kawashima, K.; Osaka, I.; Takimiya, K. Effect of Chalcogen Atom on the Properties of Naphthobischalcogenadiazole-Based π-Conjugated Polymers. *Chem. Mater.* **2015**, *27*, 6558−6570.
(40) Gu, C. L.; Hu, W. P.; Yao, J. N.; Fu, H. B. Naphthalenediimide-Benzothiadiazole Copolymer Semiconductors: Rational Molecular Design for Air-Stable Ambipolar Charge Transport. *Chem. Mater.* **2013**, *25*, 2178−2183.
(41) Nielsen, C. B.; Turbiez, M.; McCulloch, I. Recent Advances in the Development of Semiconducting DPP−Containing Polymers for Transistor Applications. *Adv. Mater.* **2013**, *25*, 1859−1880.
(42) Qiao, Y. L.; Guo, Y. L.; Yu, C. M.; Zhang, F. J.; Xu, W.; Liu, Y. Q.; Zhu, D. B. Diketopyrrolopyrrole-Containing Quinoidal Small Molecules for High-Performance, Air-Stable, and Solution-Processable n-Channel Organic Field-Effect Transistors. *J. Am. Chem. Soc.* **2012**, *134*, 4084−4087.
(43) Huang, H.; Chen, Z.; Ortiz, R. P.; Newman, C.; Usta, H.; Lou, S.; Youn, J.; Noh, Y. Y.; Baeg, K. J.; Chen, L. X.; Facchetti, A.; Marks, T. J. Combining Electron-Neutral Building Blocks with Intramolecular "Conformational Locks" Affords Stable, High-Mobility p-and n-Channel Polymer Semiconductors. *J. Am. Chem. Soc.* **2012**, *134*, 10966−10973.
(44) Lei, T.; Xia, X.; Wang, J.-Y.; Liu, C. J.; Pei, J. Conformation Locked" Strong Electron-Deficient Poly(p-phenylene vinylene) Derivatives for Ambient-Stable n-Type Field-Effect Transistors: Synthesis, Properties, and Effects of Fluorine Substitution Position. *J. Am. Chem. Soc.* **2014**, *136*, 2135−2141.
(45) Yum, S.; An, T. K.; Wang, X.; Lee, W.; Uddin, M. A.; Kim, Y. J.; Nguyen, T. L.; Xu, S.; Hwang, S.; Park, C. E.; Woo, H. Y. Benzotriazole-Containing Planar Conjugated Polymers with Noncovalent Conformational Locks for Thermally Stable and Efficient Polymer Field-Effect Transistors. *Chem. Mater.* **2014**, *26*, 2147−2154.
(46) Mao, Z. P.; Zhang, W. F.; Huang, J. Y.; Shi, K. L.; Gao, D.; Chen, Z. H.; Yu, G. High-Performance Polymer Field-Effect Transistors Fabricated with Low-Bandgap DPP-Based Semiconducting Materials. *Polym. Chem.* **2015**, *6*, 6457−6464.
(47) Zhang, W. F.; Zheng, N. H.; Wei, C. Y.; Huang, J. Y.; Gao, D.; Shi, K. L.; Xu, J.; Yan, D. H.; Han, Y. C.; Yu, G. Vinylidenedithiophenmethyleneoxindole: A Centrosymmetric Building Block for Donor−Acceptor Copolymers. *Polym. Chem.* **2016**, *7*, 1413−1421.
(48) Zhang, W. F.; Shi, K. L.; Huang, J. Y.; Gao, D.; Mao, Z. P.; Li, D. Z.; Yu, G. Fluorodiphenylethene-Containing Donor−Acceptor Conjugated Copolymers with Noncovalent Conformational Locks for Efficient Polymer Field-Effect Transistors. *Macromolecules* **2016**, *49*, 2582−2591.
(49) Jackson, N. E.; Savoie, B. M.; Kohlstedt, K. L.; Olvera de la Cruz, M.; Schatz, G. C.; Chen, L. X.; Ratner, M. A. Controlling Conformations of Conjugated Polymers and Small Molecules: The Role of Nonbonding Interactions. *J. Am. Chem. Soc.* **2013**, *135*, 10475−10483.
(50) Terblans, Y. M.; Marita Roos, H.; Lotz, S. Synthesis, Characterization and Decomposition Patterns for Thienylene Bridged Dinuclear Biscarbene Complexes of Manganese and Chromium in Refluxing Carbon Disulphide and Acetone. *J. Organomet. Chem.* **1998**, *566*, 133−142.

DOI: 10.1021/acs.macromol.6b01510
Macromolecules XXXX, XXX, XXX−XXX

(51) Frisch, M. J.; Trucks, G. W.; Schlegel, H. B.; Scuseria, G. E.; Robb, M. A.; Cheeseman, J. R.; Montgomery, Jr., J. A.; Vreven, T.; Kudin, K. N.; Burant, J. C.; Millam, J. M.; Iyengar, S. S.; Tomasi, J.; Barone, V.; Mennucci, B.; Cossi, M.; Scalmani, G.; Rega, N.; Petersson, G. A.; Nakatsuji, H.; Hada, M.; Ehara, M.; Toyota, K.; Fukuda, R.; Hasegawa, J.; Ishida, M.; Nakajima, T.; Honda, Y.; Kitao, O.; Nakai, H.; Klene, M.; Li, X.; Knox, J. E.; Hratchian, H. P.; Cross, J. B.; Bakken, V.; Adamo, C.; Jaramillo, J.; Gomperts, R.; Stratmann, R. E.; Yazyev, O.; Austin, A. J.; Cammi, R.; Pomelli, C.; Ochterski, J. W.; Ayala, P. Y.; Morokuma, K.; Voth, G. A.; Salvador, P.; Dannenberg, J. J.; Zakrzewski, V. G.; Dapprich, S.; Daniels, A. D.; Strain, M. C.; Farkas, O.; Malick, D. K.; Rabuck, A. D.; Raghavachari, K.; Foresman, J. B.; Ortiz, J. V.; Cui, Q.; Baboul, A. G.; Clifford, S.; Cioslowski, J.; Stefanov, B. B.; Liu, G.; Liashenko, A.; Piskorz, P.; Komaromi, I.; Martin, R. L.; Fox, D. J.; Keith, T.; Al-Laham, M. A.; Peng, C. Y.; Nanayakkara, A.; Challacombe, M.; Gill, P. M. W.; Johnson, B.; Chen, W.; Wong, M. W.; Gonzalez, C.; Pople, J. A. *Gaussian 03*, Revision C.02; Gaussian, Inc.: Wallingford, CT, 2004.

(52) Lei, T.; Dou, J. H.; Pei, J. Influence of Alkyl Chain Branching Positions on the Hole Mobilities of Polymer Thin-Film Transistors. *Adv. Mater.* **2012**, *24*, 6457−6461.

(53) Li, Y.; Singh, S. P.; Sonar, P. A High Mobility p-Type DPP−Thieno[3,2-*b*] thiophene Copolymer for Organic Thin-Film Transistors. *Adv. Mater.* **2010**, *22*, 4862−4866.

(54) Jackson, N. E.; Kohlstedt, K. L.; Savoie, B. M.; Olvera de la Cruz, M.; Schatz, G. C.; Chen, L. X.; Ratner, M. A. Conformational Order in Aggregates of Conjugated Polymers. *J. Am. Chem. Soc.* **2015**, *137*, 6254−6262.

(55) Rivnay, J.; Steyrleuthner, R.; Jimison, L. H.; Casadei, A.; Chen, Z. H.; Toney, M. F.; Facchetti, A.; Neher, D.; Salleo, A. Drastic Control of Texture in a High Performance n-Type Polymeric Semiconductor and Implications for Charge Transport. *Macromolecules* **2011**, *44*, 5246−5255.

DOI: 10.1021/acs.macromol.6b01510
Macromolecules XXXX, XXX, XXX−XXX

View publication stats